Solid-State Structures and Racemization of Lithiated *Schöllkopf*'s Bis[Lactim Ether]

by **Philip C. Andrews***[a]), **Melissa Maguire**[a]), and **Esteban Pombo-Villar**[b])

[a]) School of Chemistry, Monash University, P.O. Box 23, Clayton, Melbourne, Vic. 3800, Australia
[b]) Preclinical Research, *Novartis Pharma Ltd.*, CH-4002 Basel

Dedicated to Professor *Dieter Seebach* on the occasion of his 65th birthday

Addition of the respective *Lewis* base donors PMDTA and HMPA to lithiated *Schöllkopf*'s bis[lactim ether] (= 3,6-diethoxy-2,5-dihydro-2-isopropylpyrazine) results in the formation of the monomeric PMDTA complex (*R*)-(**4**) ($P2_12_12_1$, orthorhombic) and the dimeric HMPA complex (*R*,*S*)-**3** ($P\bar{1}$, triclinic), as determined by single-crystal X-ray crystallography. Complex **3** was always found in racemic form, while complex **4** was enantiomerically pure. The racemization process that leads to the HMPA complex (*R*,*S*)-**3** was investigated and found to be independent of the temperature at which either lithiation or addition of the *Lewis* base occurs.

1. Introduction. – Lithiated *Schöllkopf*'s bis[lactim ethers] have proved invaluable reagents in the synthesis of many biologically active compounds [1] and of non-proteinogenic amino acids [2]. More recent, however, is their application in the formation of phosphobutanoic acids by conjugate addition to propenylphosphonates [3]. Highly stereoselective reactions of this type are strongly affected by the presence of varying *Lewis* donors that allow the formation of different aggregation states in solution. Studying such complexes can, thus, be integral to the understanding of the stereochemistry involved in such transformations [4]. We have undertaken a solid- and solution-state study of metallated complexes of the double lactim ether (*R*)-3,6-diethoxy-2,5-dihydro-2-isopropylpyrazine (**1**). The only so far characterized lithiated compound of this type is compound **2**, which was derived form racemic cyclo-[Ala_2] obtained from THF/hexane solution. Compound **2** is a noncentrosymmetric dimer, with two unique Li-atoms and three THF molecules [5].

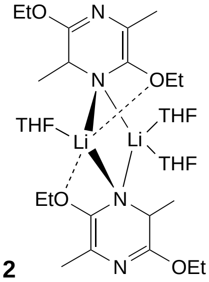

2

Here, we would like to present the crystal structures of the two HMPA[1]) and PMDTA complexes **3** and **4**, which were prepared according to the *Scheme*.

Scheme

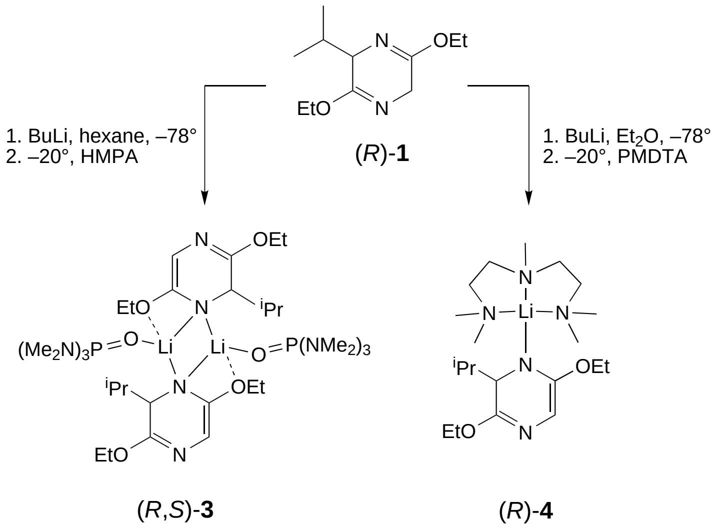

2. Results and Discussion. – The addition of BuLi to (*R*)-**1** in hexane at -78° first leads to a pale yellow solution. Upon slowly warming this solution to room temperature over several hours, a yellow precipitate begins to form at *ca.* -30°, which indicates the point where lithiation of the bis[lactim ether] occurs in the absence of *Lewis* donors. When this reaction is carried out at room temperature, the bright yellow precipitate forms immediately. In an attempt to obtain crystalline products, various typical *Lewis* donors were added to the yellow suspensions of lithiated (*R*)-**1**. The addition of 1.2 equiv. of HMPA produced a pale brown solid that separated from the slightly orange solution. After removing the hexane and slowly adding toluene, a red-brown solution was obtained from which small crystals of adduct **3** were isolated on cooling to 4° overnight. Structural characterization by X-ray diffraction revealed that **3** is dimeric, as shown in *Fig. 1*, and that an unexpected racemization of the bis[lactim ether] had occurred. So far, we have not been able to obtain crystals of either the THF or Et_2O adducts of $\mathbf{1}\cdot$Li, which would be the classical solvents of choice. However, HMPA complexes are also interesting targets for two reasons. First, the HMPA $P{=}O$ bond is similar to the phosphonate systems we are interested in, second, the addition of HMPA to the lithiated bis[lactim ether] in its conjugate to prop-1-enyl phosphonates generally gives rise to a negligible diastereoisomeric excess [3].

Upon addition of the tridentate N donor PMDTA to a yellow suspension of (*R*)-**1** at room temperature, a red oil separated from the hexane layer. The latter was removed

---

[1]) HMPA stands for hexamethylphosphoric triamide, PMDTA is *N,N,N′,N′,N″*-pentamethyldiethylenetriamine.

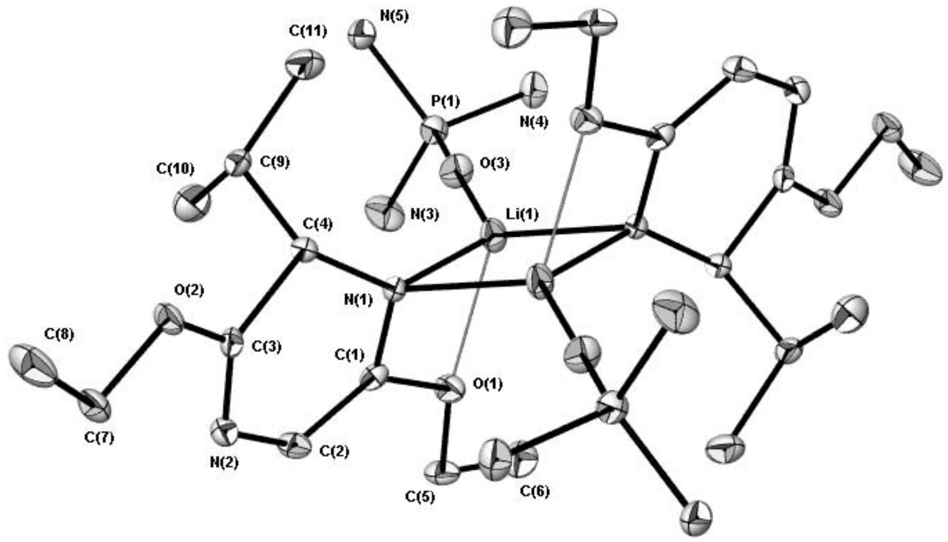

Fig. 1. *Molecular structure of the HMPA complex* **3**. Thermal ellipsoids are shown at 50% probability. All H-atoms are omitted for clarity. Selected bond distances (Å) for one dimer: N(1)–Li(1) 2.047(5); N(1)–Li(1a) 2.089(5); Li(1a)–O(1) 2.095; Li(1)–O(3) 1.836(5); N(1)–C(1) 1.347(3); N(1)–C(4) 1.459(3); N(1)–Li(1)–O(3) 126.1(2). Selected bond angles (°): Li(1)–N(1)–C(1) 117.0(2); Li(1)–N(1)–C(4) 114.0(2); Li(1)–O(3)–P(1) 173.9(2); Li(1)–N(1)–Li(1a) 76.9(2); N(1)–Li(1)–N(1a) 103.1; N(1)–C(1)–O(1) 109.1(2); C(1)–O(1)–Li(1a) 90.6(2).

and the oily residue dissolved in warm Et$_2$O. To simplify the process, lithiation was directly performed in Et$_2$O at -60°. From the initial pale yellow solution, a brownish precipitate separated upon slowly warming the mixture to ambient temperature. Addition of PMDTA (1 equiv.) then led to a dark yellow-brown solution from which, on storage overnight at 4°, yellow crystals separated, which were washed with cold Et$_2$O and identified by single-crystal X-ray diffraction as the monomeric PMDTA adduct **4** (*Fig. 2*). In contrast to the HMPA adduct **3**, the crystal structure of **4** did not indicate any racemization. Optical rotation measurements of hydrolyzed samples confirmed that the lactim ether **1** in the HMPA complex had indeed completely racemized while the PMDTA-derived compound had retained its original configuration.

Often, racemization is both solvent and temperature dependent. In an attempt to understand the dramatically different action of the two above *Lewis* bases, we performed a series of experiments conducted at different temperatures. First, BuLi was added to (*R*)-**1** at -78°, and the mixture was allowed to slowly warm to ambient temperature. As previously noted, metallation does not occur below *ca.* -30°. Once the precipitate had formed, the appropriate *Lewis* base was added at *ca.* -20°, before warming was continued. In a second experiment, both lithiation and *Lewis* base addition were carried out at ambient temperature (22°). The results of these two types of experiments are summarized in *Table 1*.

Next, we studied **1** · Li, which forms a yellow precipitate in hexane in the absence of any *Lewis* base, both at low and ambient temperature. The crude metallation products were separated, washed twice with hexane, dried *in vacuo*, and stored in a glove box.

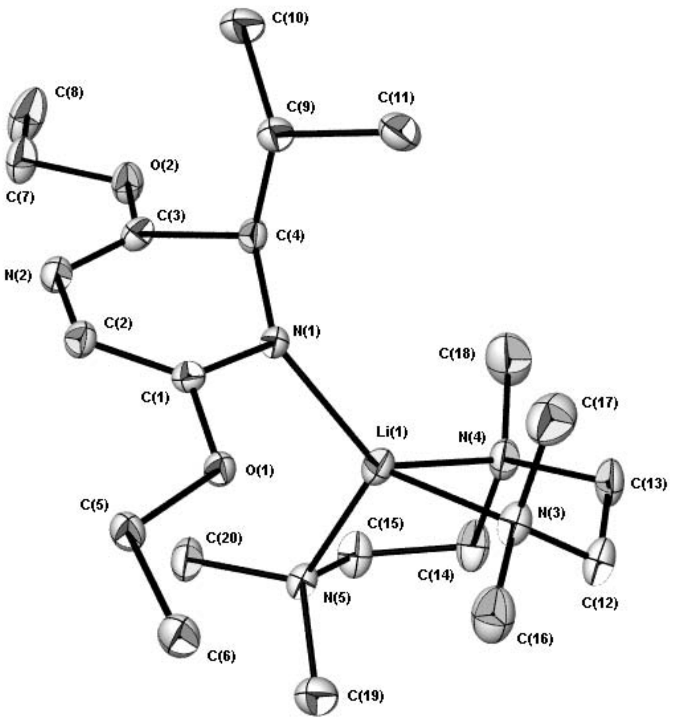

Fig. 2. *Molecular structure of the PMDTA complex* **4**. Thermal ellipsoids are shown at 50% probability. All H-atoms are omitted for clarity. Selected bond distances (Å): N(1)–Li(1) 1.965(3); Li(1)–N(3) 2.158(3); Li(1)–N(4) 2.185(3); Li(1)–N(3) 2.146(3); N(1)–C(1) 1.338(2); N(1)–C(4) 1.468(2); C(3)–O(2) 1.377(2); C(1)–O(1) 1.397(2). Selected bond angles (°): Li–N(1)–C(1) 107.5(1); Li(1)–N(1)–C(4) 139.6(1); N(1)–C(1)–O(1) 110.7(1); C(1)–N(1)–C(4) 111.8(1)

Table 1. *Optical Rotations of the Ligand* **1** *and the Respective Hydrolyzed Samples of the HMPA and PMDTA Complexes* **3** *and* **4** *Obtained under Different Reaction Conditions*

Compound	*T* [°]	Solvent	Conc. [mM]	Optical Rotation $[\alpha]^{22}_{D}$ [°]
1	–	–	10.0	– 78.8
1·Li	– 78	hexane	9.6	– 24.5
1·Li	r.t.	hexane	9.5	– 22.2
(*R*)-(**4**)	– 20	hexane/Et_2O	9.8	– 27.8
(*R*)-(**4**)	r.t.	hexane/Et_2O	9.6	– 24.9
(*R*,*S*)-**3**	– 20	hexane	9.5	– 1.3
(*R*,*S*)-**3**	r.t.	hexane/toluene	9.5	– 0.3

Unfortunately, they proved to be only sparingly soluble in (D_6)benzene; yet, we were able to obtain weak ^{1}H-NMR spectra. These spectra were not only identical, they also suggested that competitive deprotonation at the chiral C-atom (one possible source of racemization) does not occur at this stage, and, moreover, that the conversion to an amide, as observed in the solid-state structures, had also not yet taken place. In order to obtain better resolutions, the compounds were dissolved in (D_6)benzene/(D_8)THF 1:1. The ^{1}H-NMR signal of the allylic proton of **1** · Li was now observed in both spectra at *ca.* 5.5 ppm, indicating that the conversion of the lithium alkyl to a lithium amide, as seen in **3** and **4**, is highly solvent dependent. Next, the optical rotations of two hydrolyzed samples dissolved in toluene were determined. Practically identical rotations were found, which confirmed the isomeric purity of both probes suggesting that the temperature at which lithiation occurs is largely irrelevant.

Addition of HMPA at low temperature to **1** · Li gave an orange solution from which pale yellow crystals were directly obtained upon warming. However, when the same reaction was performed at room temperature, an oily precipitate was formed that required the addition of toluene to be completely dissolved. Crystal growth took place at $-25°$ over several days, but there was always an accompanying viscous dark red oil. Surprisingly, optical rotation measurements of hydrolyzed samples dissolved in toluene indicated that both probes had completely racemized. We are, as yet, unsure what the red oil might be. However, we noticed that crystals of the HMPA complex **3** have a tendency to turn dark red on the surface when stored at room temperature. This surface material appears to be oily and, over time, tiny crystals completely 'melt'. At present, we believe that oxygen contamination and some further reactions have occurred in these cases.

To obtain crystalline samples of the PMDTA complex **4**, Et_2O had to be added to the crude products after removal of the hexane used in the metallation. Interestingly, crystals obtained from samples that had been prepared at room temperature were bright yellow in appearance, while those obtained at $-20°$ were colorless. In contrast to crystals of type **3**, which displayed an effective zero rotation, both sets of hydrolyzed PMDTA complexes **4** gave rise to almost identical degrees of rotation – similar in magnitude as the uncomplexed **1** · Li samples (*cf. Table 1*). While this preliminary study is not comprehensive, it nevertheless indicates that HMPA is the cause for the observed racemization, a process that seems to be largely temperature-independent. At least, we have not been able to isolate nonracemic crystals of the HMPA complex so far. To ensure that our observation is valid not only for selected single crystals, we also analyzed powdered (noncrystalline) samples obtained from the above reaction mixtures. However, qualitatively, the same results were obtained.

Although more bulky than THF and with a higher partial charge on the O-atom (promoting a higher degree of bonding flexibility), the structures adopted by HMPA adducts of lithium amides can often be similar in construction[2]). It was very interesting that the crystal structure of **3** is significantly different from that of **2**, although both compounds display many features common to lithium amides coordinated by a single monodentate donor (*e.g.*, dimeric structure, almost planar, rhomboidal, or square four-membered $(LiN)_2$ ring, with *trans*-oriented substituents [7]).

While the solid-state structure of **2** displays three THF molecules and two nonidentical Li-atoms on an approximate C_2-axis, the asymmetric unit of **3** contains two crystallographically independent dimers (triclinic, space group $P1$), with only one external *Lewis* donor atom per metal center (*Table 2*). This probably reflects the increased steric requirements of HMPA as compared to THF. In contrast to **4**, both **2**

---

[2]) For example, THF- and HMPA-complexed lithium dibenzylamide [6].

and **3** posses a relatively short Li,O(Et) distance that allows the Li to increase its coordination environment. However, in compound **2**, there is only one of the two Li-atoms involved and it binds to *two* EtO groups. This is mirrored in a Li(1)–O(1) and Li(1)–O(4) distance of 2.095(5) and 2.087(5) Å for **3** compared to only 2.25(1) Å in **2**. The Li–O(P) bonds in **3** (1.838(5) and 1.853(5) Å) are, as expected, the shortest, which reflects the significant partial charge on oxygen and the consequent minimized geometrical constraints in forming the Li–O bond. This flexibility results mainly from electrostatic interactions and allows the Li center, which is located on the same side of the ring as the i-Pr group, to maximize bonding and to minimize unfavorable steric interactions. This results in the pyrazine rings being tilted away by *ca.* 37° from a perpendicular position relative to the $(LiN)_2$ ring. The planar $(LiN)_2$ rings themselves are rhomboidal, with internal N–Li–N angles of 103.44° for Li(2) and 103.13° for Li(1), together with Li–N distances of 2.035(5) and 2.122 Å (Li(2)–N(6)), as well as 2.089 and 2.047 Å within both dimers (Li(1)–N(1)).

Table 2. *Crystallographic Data of Compounds* **3** *and* **4**

Compound	**3**	**4**
Empirical formula	$C_{34}H_{74}N_{10}O_6P_2Li_2$	$C_{20}H_{42}N_5O_2Li$
Formula weight	794.85	391.53
Crystal temp. [K]	123	123
Crystal system	triclinic	orthorhombic
Lattice parameters:		
$2\theta_{max}$ [°]	56.74	56.56
a [Å]	11.241(2)	10.113(2)
b [Å]	14.029(2)	14.153(2)
c [Å]	15.298(3)	16.925(3)
α [°]	93.65(3)	90
β [°]	107.67(3)	90
γ [°]	96.14(3)	90
V [Å^3]	2273.7(8)	2422.5(8)
Space Group	$P1$	$P2_12_12_1$
Z	2	4
D_x [g cm^{-3}]	1.161	1.074
μ [cm^{-1}]	0.98	0.98
N_{unique}	10630	6001
R_w	0.119	0.090
R_1 [$I > 2\sigma(I)$]	0.068	0.043
Goodness-of-fit	1.017	1.064

Complex **4** crystallizes in an orthorhombic space group ($P2_12_12_1$) with four molecules in the unit cell. Li is bonded directly to the N-atom adjacent to the chiral C-atom of the dihydropyrazine ring and to the three PMDTA N-atoms, with distances of 1.965(3) Å for Li(1)–N(1), and 2.158(3), 2.185(3), and 2.146(3) Å for Li(1)–N(*n*) (*n* = 3, 4, 5). These bond lengths are typical for distorted tetrahedral arrangements at the Li center. As expected, and in agreement with calculated structures of monomeric **1** · Li coordinated to three donor atoms [3], the i-Pr group is located on the opposite side of the pyrazine ring relative to the metal, and the Li center is not in close bonding distance with the nearest O-atom (Li(1)–O(1) = 2.568 Å). However, the Li-atom does not lie symmetrically between C(1) and C(4), but is angled towards O(1), thereby protruding by 14.7° from the plane defined by C(1)–N(1)–C(4), which minimizes steric interactions.

Variable-temperature ^{1}H- and ^{13}C-NMR spectra were recorded for the two complexes **3** and **4** in (D_8)toluene in the range of +30 to −80°. At 30° in solution, the structure of the two compounds are probably more 'complicated' than in the solid state. The main differences in the spectra of **3** and **4**, apart from the different chelating donor molecules, appear in the region of the CH_2O resonances of the lactim ether groups. From the crystal structures and our general experience, there are two distinct ether moieties: one lies close to the Li-center and gives rise to signals at higher frequency, while the opposite is true for the other. Thereby, the CH_2O H-atoms located closer to the Li-atom appear as two distinct signals at 4.49 and 4.37 ppm in **4**, and at 4.40 and 4.15 ppm in **3**.

Interestingly, while it is quite clear from the solid-state structure of **3** that this ether O-atom is coordinated to Li, it is not so unambiguous in **4**, as possibly reflected by the differential chemical shifts of the two geminal H-atoms in each complex (0.12 and 0.25 ppm in **4** *vs.* **3**). All ether methylene protons in the chiral metallated complex **4** are located in different electronic environments, with the lower-frequency CH_2O signals also being quite distinct (3.88 and 3.79 ppm), while those in the racemic complex **3** are averaged (3.78 ppm). This does not change in the spectra recorded at lower temperatures. Even the more distant Me protons of the ether moieties display quite different chemical shifts. In **4**, they are nicely separated at 1.36 and 1.12 ppm at 30°, and 1.42 and 1.02 ppm at −60°, respectively. Unfortunately, in the racemic compound **3** part of the signals are covered by i-Pr *doublets*. In the case of **4**, it could be possible that both close-contact and solvent-separated ion pairs form in solution and allow the Li to relocate such that both pyrazine N-atoms and their closest related ether O-atoms bond to the Li-atom. While in the ^{1}H-NMR spectra of **3** very little change is observed with temperature, the PMDTA signals of **4** first broaden and then split between 0 and −45°, before they sharpen again at −60°. However, even then, no distinct splitting of the broad *singlets* occurs, of which there are at least six with irregular integration values. ^{1}H,^{1}H-correlation spectra did not help to solve this inconsistency. Despite the fact that there are always two signals apparent for the CH_2O H-atoms closest to the Li-center, it could also be possible that the tridentate PMDTA ligand does not permanently coordinate to the Li-atom with all of its three N-atoms. This phenomenon has been observed both in the solid state [8] and in solution [9] of organolithium complexes. However, ^{7}Li-NMR spectra indicated only one type of chemical environment with respect to Li, even at −80°. We, therefore, conclude that the crystallographically-determined solid-state structures are largely retained in solution and that the various PMDTA signals arise from the chiral environment.

3. Conclusions. – We prepared two different Li complexes **3** and **4** from metallated *Schöllkopf*'s bis[lactim ether] (**1**) and HMPA as well as PMDTA, respectively, and successfully determined solid-state structures. The HMPA complex **3** is dimeric in the solid state, while the corresponding PMDTA complex **4** is monomeric and, in contrast to **3**, retains its optical activity during complex formation. Our studies clearly indicate that HMPA as such (rather than temperature effects) are primarily responsible for the observed racemization. However, the temperature at which the *Lewis* base is added to the metallated lactim ether strongly affects the 'quality' of the reagent, as expected. At ambient temperatures, the target complexes are present as oils *and* crystals, while addition of the reagent at low temperatures leads to crystalline material only.

Experimental Part

General. All reactions were performed using standard *Schlenk* techniques. All other manipulations were done in a recirculating glove box kept under high-purity Ar. All solvents were refluxed over Na/K alloy prior to use and stored over molecular sieves (4 Å). HMPA and PMDTA were refluxed over CaH_2, distilled, and also stored over molecular sieves (4 Å). BuLi (1.6M in hexanes) was purchased from *Merck-Schuchardt*. (*R*)-3,6-Diethoxy-2,5-dihydro-2-isopropylpyrazine (**1**) was synthesized in the *Novartis* laboratories. ^{1}H-NMR Spectra were recorded on a *Bruker DRX-400* spectrometer, chemical shifts δ in ppm rel. to $SiMe_4$. Elemental analyses were carried out by *CMAS*, Australia. Optical rotation measurements were performed on a *PolAAr 2001* apparatus.

Crystal Structure Determinations. Single crystals of **3** and **4** of good quality were coated in oil and mounted on a fibre. Data were collected on an *Enraf Nonius KappaCCD* at 123 K with MoK_α radiation ($\lambda = 0.71073$ Å). Structures were solved by direct methods (SHELXS 97) [10] within X-SEED [11] and refined by full-matrix least-squares on F^2. H-atoms were placed in calculated positions (C−H distance: 0.95 Å) and included in the final least-squares refinement. All other atoms were located and refined anisotropically. Crystallographic data (excluding structure factors) have been deposited with the *Cambridge Crystallographic Data Centre* (*CCDC*) as supplementary publication numbers *CCDC* 173805 (compound **3**) and *CCDC* 173806 (compound **4**). Copies of the data can be obtained, free of charge, on application to *CCDC*, 12 Union Road, Cambridge, CB21EZ, UK (fax: +44(1223)336033, e-mail: deposit@ccdc.cam.ac.uk).

Syntheses. Complex **3**. A soln. of **1** (5 mmol, 1.06 g) in anh. hexane (10 ml) was cooled to −78°, and BuLi (5 mmol, 3.13 ml) in hexanes was added dropwise. The pale yellow soln. was allowed to slowly warm to −20°, by which time a yellow precipitate had formed. HMPA (6 mmol, 1.04 ml) was added and the mixture was allowed to warm to r.t., which led to a pale brown solid immersed in an orange soln. The mixture was concentrated *in vacuo* and dissolved in toluene by gentle heating. Upon standing overnight at r.t., pale yellow crystals were obtained, which were filtered off, washed with hexane, and dried *in vacuo*. Yield: 71%. M.p. 126–128°. ^{1}H-NMR (400 MHz, (D_8)toluene, 30°): 5.25 (*s*, C=C(H)N); 4.40 (*m*, 1 H, CH_2O); 4.15 (*m*, 1 H, CH_2O); 4.11 (br. *d*, Me$_2$C*H*); 3.78 (*m*, CH_2O); 2.36 (*d*, 18 H, HMPA); 2.24 (*dq*, CH); 1.28 (*t*, *Me*CH$_2$O); 1.20 (*m*, *Me*$_2$CH, *Me*CH$_2$O). ^{13}C-NMR (100 MHz, (D_8)toluene, 30°): 162.6 (C_q); 146.5 (C_q); 79.4 (C=C−N); 64.5 (O−C=C); 59.6 (CH); 47.1 (CH_2O); 36.6 (HMPA); 31.9 (Me$_2$*C*); 20.0 (*Me*$_2$C); 15.5 (*Me*$_2$C); 14.5 (*Me*CH$_2$O). Anal. calc. for $C_{17}H_{38}LiN_5O_3P$: C 51.3, H 9.6, N 17.6; found: C 50.8, H 10.8, N 16.9.

Complex **4**: A soln. of **1** (5 mmol, 1.06 g) in anh. Et_2O (8 ml) was cooled to −78°, and BuLi (5 mmol, 3.13 ml) in hexanes was added dropwise. The yellow soln. was allowed to slowly warm to −20°, by which time a light brown precipitate had formed. PMDTA (5 mmol, 1.04 ml) was added, and the mixture was allowed to warm to r.t. Gentle heating produced a golden soln. from which colorless crystals were separated overnight at 4°. The crystals were filtered off, washed with hexane, and dried *in vacuo*. Yield: 83%. M.p. 143–145°. ^{1}H-NMR (400 MHz, (D_8)toluene, 30°): 5.35 (*s*, C=C(H)N); 4.49 (*m*, 1 H, CH_2O); 4.37 (*m*, 1 H, CH_2O); 3.88 (*m*, 2 H, CH_2O, Me$_2$C*H*); 3.79 (*m*, 1 H, CH_2O); 2.29 (*dq*, CH); 2.01 (*s*, MeN); 1.99 (*s*, 4 MeN); 1.84 (br. *s*, 4 CH_2N); 1.36 (*t*, *Me*CH$_2$O); 1.24 (*d*, Me); 1.19 (*d*, Me); 1.12 (*t*, *Me*CH$_2$O). ^{7}Li-NMR (155.5 MHz, (D_8)toluene): 0.61 (at 30°); 0.65 (at −80°). ^{13}C-NMR (100 MHz, (D_8)toluene, 30°): 164.8 (C_q); 145.3 (C_q); 79.9 (N−*C*=C); 67.8 (C=*C*−O); 62.0 (CH_2O); 59.3 (CH_2N); 56.2 (CH_2N); 47.5 (MeN); 34.0 (Me$_2$*C*); 21.9 (*Me*$_2$C); 17.8 (CH_2O). Anal. calc. for $C_{20}H_{42}LiN_5O_2$: C 61.4, H 10.8, N 17.9; found: C 62.1, H 10.0, N 17.3.

REFERENCES

[1] C. Ma, X. Lui, S. Yu, S. Zhao, J. M. Cook, *Tetrahedron Lett.* **1999**, *40*, 657; M. Lange, P. M. Fischer, *Helv. Chim. Acta* **1998**, *81*, 2053; T. Gan, J. M. Cook, *Tetrahedron Lett.* **1997**, *38*, 1301; M. Ruiz, V. Ojea, J. M. Quintela, *Tetrahedron Lett.* **1996**, *37*, 5743.

[2] R. M. Williams, in 'Synthesis of Optically Active α-Amino Acids', Organic Chemistry Series, Vol. 7, Eds. J. M. Balwin, P. D. Magnus, Oxford, 1989; U. Schöllkopf, D. Pettig, E. Schulze, M. Klinge, E. Egert, B. Benecke, M. Noltmeyer, *Angew. Chem., Int. Ed.* **1988**, *27*, 1194; D. Pettig, U. Schöllkopf, *Synthesis* **1988**,

173; U. Schöllkopf, J. Schröder, *Liebigs Ann. Chem.* **1988**, *87*; U. Schöllkopf, W. Kühnle, E. Egert, M. Dyrbusch, *Angew. Chem., Int. Ed.* **1987**, *26*, 480; U. Schöllkopf, D. Pettig, U. Busse, E. Egert, M. Dyrbusch, *Synthesis* **1986**, 737; U. Schöllkopf, *Pure Appl. Chem.* **1983**, *55*, 1799.

[3] V. Ojea, M. Ruiz, G. Shapiro, E. Pombo-Villar, *J. Org. Chem.* **2000**, *65*, 1984; V. Ojea, M. Carmen Fernández, M. Ruiz, J. M. Quintela, *Tetrahedron Lett.* **1996**, *37*, 5801.

[4] D. Seebach, *Angew. Chem., Int. Ed.* **1988**, *27*, 1624.

[5] D. Seebach, W. Bauer, J. Hansen, T. Laube, W. B. Schweizer, J. D. Dunitz, *J. Chem. Soc., Chem. Commun.* **1984**, 853.

[6] D. Barr, W. Clegg, R. E. Mulvey, R. Snaith, *J. Chem. Soc., Chem. Commun.* **1984**, 288; P. C. Andrews, D. R. Armstrong, D. R. Baker, R. E. Mulvey, W. Clegg, L. Horsburgh, P. A. O'Neil, D. Reed, *Organometallics* **1995**, *14*, 427.

[7] R. E. Mulvey, *Chem. Soc. Rev.* **1998**, *27*, 339; R. E. Mulvey, *Chem. Soc. Rev.* **1991**, *20*, 167; K. Gregory, P. v. R. Schleyer, R. Snaith, *Adv. Inorg. Chem.* **1991**, *37*, 47.

[8] P. C. Andrews, W. Clegg, R. E. Mulvey, *Angew. Chem., Int. Ed.* **1990**, *29*, 1440; P. Jutzi, E. Schlueter, E. Krueger, S. Pohl, *Angew. Chem., Int. Ed.* **1990**, *22*, 994.

[9] H. J. Reich, W. S. Goldenberg, B. Ö. Gudmundsson, A. W. Sanders, K. J. Kulicke, K. Simon, I. A. Guzei, *J. Am. Chem. Soc.* **2001**, *123*, 8067; H. J. Reich, B. Ö. Gudmundsson, *J. Am. Chem. Soc.* **1996**, *118*, 6074; G. Fraenkel, A. Chow, W. R. Winchester, *J. Am. Chem. Soc.* **1990**, *112*, 6190.

[10] G. M. Sheldrick, SHELXS97, Program for the Solution of Crystal Structures, Göttingen, Germany, 1997.

[11] L. J. Barbour, X-SEED, Graphical Interface for the SHELX Program Suite, University of Missouri, 1999.

Received March 18, 2002